NASA TECHNICAL MEMORANDUM

NASA TM X- 72629

COPY NO.

NASA TM X-72629

A SIMULATION OF SYNTHETIC APERTURE RADAR IMAGING OF OCEAN WAVES

Calvin T. Swift

October 29, 1974 .

NATIONAL AERONAUTICS AND SPACE ADMINISTRATION

LANGLEY RESEARCH CENTER, HAMPTON, VIRGINIA 23665

1. Report No.	2. Government Accession No.	3. Recipient's Catalog No.
NASA TM X-72629		

4. Title and Subtitle	5. Report Date
A Simulation of Synthetic Aperture Radar Imaging of Ocean Waves	October 29, 1974
	6. Performing Organization Code
7. Author(s)	8. Performing Organization Report No.
Calvin T. Swift	
9. Performing Organization Name and Address	10. Work Unit No.
NASA Langley Research Center Hampton, VA 23665	11. Contract or Grant No.
12. Sponsoring Agency Name and Address	13. Type of Report and Period Covered
National Aeronautics & Space Administration Washington, DC 20546	NASA Technical Memorandum
	14. Sponsoring Agency Code

15. Supplementary Notes

Paper presented at the 1974 USNC/URSI Meeting, Boulder, Colorado, October 14-17, 1974

16. Abstract

A simulation of radar imaging of ocean waves with synthetic aperture techinques is presented. The modelling is simplistic from the oceanographic and electromagnetic viewpoint in order to minimize the computational problems, yet reveal some of the physical problems associated with the imaging of moving ocean waves. The model assumes: (1) The radar illuminates a one-dimensional, one harmonic ocean wave that propagates as $\sin(\frac{2\pi X}{L} - \omega t)$ where L = ocean wavelength and g - acceleration due to gravity, $\omega = \sqrt{2\pi g/L}$. (2) The scattering is assumed to be governed by geometrical optics. (3) The radar is assumed to be down-looking, with doppler processing (range processing is suppressed due to the one-dimensional nature of the problem). (4) The beamwidth of the antenna (or integration time) is assumed to be sufficiently narrow to restrict the specular points of the peaks and troughs of the wave.

The results show that conventional processing of the image gives familiar results if the ocean waves are stationary i.e., if $\omega = 0$. the specular points are resolved within the resolution element $\epsilon = \lambda H/2vT$ where λ = electromagnetic wavelength, H = aircraft altitude, v = aircraft velocity and T = integration time for the synthetic aperture. When the ocean wave dispersion relationship $\omega = \sqrt{2\pi g/L}$ is satisfied, the image is "smeared" due to the motion of the specular points over the integration time. In effect, the image of the ocean is transferred to the near field of the synthetic aperture.

17. Key Words (Suggested by Author(s)) (STAR category underlined)	18. Distribution Statement
Communications Electromagnetic Rough Surface Scattering, Synthetic Aperture Radar, Radio Oceanography	Unclassified-Unlimited

19. Security Classif. (of this report)	20. Security Classif. (of this page)	21. No. of Pages	22. Price*
Unclassified	Unclassified	12	$3.25

*Available from { The National Technical Information Service, Springfield, Virginia 22151
STIF/NASA Scientific and Technical Information Facility, P.O. Box 33, College Park, MD 20740

INTRODUCTION

A side-looking imaging radar can obtain good azimuth resolution either by utilizing a long narrow beam antenna, or by developing a "synthetic aperture" which requires a time integration of the phase of the scattered signal. The problem with using real apertures from space is that resolution of a few tens of meters requires an antenna that is a few hundred meters long. The problem with the synthetic aperture is that the ocean waves are moving as the synthetic aperture is developed. The latter problem is the subject of this paper.

The statistical theory of rough surface scattering has been used with success to define the average microwave scattering cross-section of the ocean. Such a statistical theory; however, is not appropriate for interpreting radar imagery since the scene is deterministic. Therefore, in order to analyze the synthetic aperture radar, an ocean-like surface must be generated, and the calculations of the magnitude and phase of the scattered energy must be undertaken on that particular surface.

In order to derive a closed form solution of an ocean wave image, it is assumed that the ocean wave propagates only in one direction and that the wave is monochromatic. The antenna is assumed to illuminate the surface in the near nadir direction, and geometric optics is assumed to govern the scattering process. The image is reconstructed by doppler ordering of the phases of the scattered signal. Parametric calculations are presented as a function of integration time, platform altitude to velocity ratio, ocean wavelength and electromagnetic wavelength. It is,

shown that unless the system parameters are judiciously selected serious distortion of the image can occur.

Discussion of Figures

Figure 1 shows the two-dimensional geometry for the imaging of specular points by means of doppler ordering the back-scattered electric field as the antenna beam moves over the specular points. In this figure, $\bar{R}$ is the radius vector to a point along the X-axis, H and v are the altitude and velocity of the moving platform and X_i is the position of the ith stationary specular point. The time reference is chosen so that at $t = 0$ h is the perpendicular distance to any given ith specular point.

The phase relationship for the return from the ith specular point is given by the equations in the figure, where the latter is an approximation for large h. Note that the phase contains a t^2 term due to the variable doppler shift of the specular point as it passes through the antenna beam.

Figure 2 shows the simplified system model used in this paper for the analysis of the scattered return. The received signal S_1 is mixed with a reference chirp to re-order the doppler components. The signal then goes through a low pass filter to produce S_3, whose phase depends linearly on time. This signal is then integrated over time T and squared to produce the intensity, S_4. The resultant signal S_4 is a series of sinc^2 functions of width $X_o = h/2vT$, where X_o is the resolution of the image. For analytical simplicity, a zero IF stage

which passes both positive and negative frequencies has been postulated.

Figure 3 shows a very simplistic model of a moving ocean wave that is being imaged. The wave is a single harmonic gravity wave of wave number $K = 2\pi/L$ (L = wave length) and radian frequency $\Omega = \sqrt{Kg}$, where g is the acceleration due to gravity. In this geometry, the antenna beam θ_B is assumed to be small enough so that only those specular points at normal incidence are illuminated. Therefore, reflections occur at the peaks and troughs of the ocean wave; i.e., a double harmonic is imaged. Also the amplitude of the return from each specular point is the same: only an uninteresting phase shift of 90° occurs between the peaks and troughs.

Because of the motion of the wave, the specular points will move in time in proportion to the phase velocity $v_{ph} = \sqrt{g/K}$, as given by the equation in the figure. Since $X - X_i(t)$ is squared additional terms proportional to t^2 will appear in the exponential. The time integration of signal S_3 will therefore be Fresnel integrals instead of simple sinc^2 functions.

The details of the derivation explicitly give

$$S_4{}^i = \frac{X_o}{4 v_{ph} T} \left\{ \left[C(\zeta_+^i) + C(\zeta_-^i) \right]^2 + \left[S(\zeta_+^i) + S(\zeta_-^i) \right]^2 \right\}$$

where

$$C(\zeta) + j\, S(\zeta) = \int_o^\zeta e^{\frac{j \pi u^2}{2}}\, du$$

$$\zeta_{\pm}^{i} = \sqrt{\frac{v_{ph}T}{X_o}} \left\{ 1 \pm \frac{X_o}{v_{ph}T} \left[\frac{X}{X_o} - \frac{(2i+1)\pi}{2KX_o} \right] \right\}$$

$$X_o = \frac{h}{2vT}$$

As the antenna scans off nadir, the specular points will move towards the even zero crossings of the X-axis, so that the illumination approaches a spacing equal to L, the ocean wavelength. Indeed a simple calculation shows that the specular points are identically spaced L apart when the θ, the viewing angle, is

$$\theta = \theta_c = \tan^{-1} \left(\frac{2\pi A}{L} \right)$$

There are no specular points for incidence angles greater than that given above. Therefore, the specular points occur at distances $\frac{L}{2}$ apart at nadir; and approach a spacing of L at the critical viewing angle θ_c, beyond which, they entirely disappear from view. There is no unique relationship between the amplitude and length of an ocean wave; however, the rms slope $(\overline{A/L})$ generally increases with increasing wind speed and decreasing depth of the bottom. Under these conditions, some specular returns will occur with reasonable probability for viewing angles up to 20 or 30 degrees. At greater angles of incidence, Bragg scattering will dominate.

Figure 4 shows the radar image of a "frozen" ocean wave ($v_{ph} = 0$). The value of 40 sec. for the h/v ratio is approximately the value for a high flying transonic jet aircraft. Intensity peaks occur every 20 meters, or one-half an ocean wavelength. This figure shows that the

resolution of the image improves as the integration time increases.

Figures 5-8 show how the image of a moving specular point is distorted as the integration time increases. The calculations assume that the ocean wave propagates with a phase velocity $v_{ph} = \sqrt{g\,L/2\pi}$. For $T = 0.5$ sec. (figure 5), the intensity distribution closely resembles the sinc^2 function. As T increases to 1.0 sec. (figure 6), the width of the central peak is only slightly greater than X_o, the width of the sinc^2 function. However, large side lobes are beginning to appear. When the integration time increases to 1.2 sec. (figure 7), the pair of side lobes are almost as intense as the central lobe; and severe image distortion occurs. Finally, for $T = 1.4$ seconds (figure 8), destructive interference causes a minimum to occur at the specular point position.

Figure 9 shows the distortion of the specular point image as a function of the electromagnetic wavelength λ or h/v for $L = 40$ m and $T = 1.0$ sec. With $h/v = 40$ sec., the image degrades as the electomagnetic wavelength becomes shorter than 0.5 m. A re-scaling of parameters shows that with $\lambda = .25$ m., the distortion is reduced as h/v increases. However, an increasing h/v will result in a larger value of X_o; i.e., poorer resolution.

In figure 10, $T = 1.0$ sec., $\lambda = 0.25$ m and $h/v = 40$ sec., and L is allowed to vary. As the ocean wave increases, the phase velocity also increases; and the image is distorted. On the other hand, as the ocean wavelength becomes smaller, the specular points are closer to each other and the image of a given specular point smears into the image of its

neighbor. This figure therefore implies that there is both a minimum and a maximum ocean wave that can be imaged.

Figures 11 and 12 outline methods by which the imaging of an ocean wave can be optimized. Figure 11 indicates how a distorted image may be reconstructed by hardware implementation. If the Chirp frequency is tuned by an amount equal to $1 - 2V_{ph}/V$, then the mixing and filtering of signals S_1 and S_2 results in a signal S_3, which contains no quadratic time varying phase terms. The integrated signal then becomes a sinc^2 function, and the specular point is resolved to within x_o. The difficulty is that one must know what the ocean wavelength is in order to measure it! Another difficulty is that this method will restore only one wavelength of what is generally a spectral ensemble of wavelengths.

The other method (figure 12) is to make an appropriate selection of the electromagnetic wavelength to image the range of ocean wavelengths of interest. This can be done by utilizing the two conditions given in the figure. The first criterion $x_o \leq L_{min}/4$ resolves the minimum ocean wavelength as reviewed from near nadir. The second criterion $x_o \geq v_{ph\ max}\, T$ follows from inspection of the Fresenel integral expression given earlier. Basically, the latter inequality states that a given specular point must remain within the resolution cell during the integration period. Otherwise image distortion will result. These criteria are conservative because the specular points will tend to be spaced a full wavelength apart as the viewing angle increases; and the calculations show that latter criterion can be "slightly" violated before serious image distortion occurs.

If the inequalities are replaced by equalities, and if T is eliminated, one obtains the result in the box. If h/v is fixed, this equation states that the greatest range of ocean wavelengths can be illuminated by choosing the shortest practical electromagnetic wavelength.

CONCLUDING REMARKS

Geometric optics has been used as a scattering model in order to interpret the synthetic aperture image of a moving ocean wave. The results basically show that the image of a monochromatic ocean wave will be distorted if the product of the integration time and the phase velocity of the wave exceeds the resolution of the synthetic aperture.

When the monochromatic wave is viewed in the nadir direction, specular points (images) occur at increments of one-half an ocean wavelength. As the viewing angle increases, the images occur at one-wavelength intervals and then disappear with increasing viewing angle.

Numerical techniques can be used to generate a surface which spectrally resembles an ocean wave, and calculations performed within 20 to 30° of nadir should be physically meaningful. At steeper viewing angles, the model must include the Bragg Scattering Mechanism.

IMAGING RADAR GEOMETRY

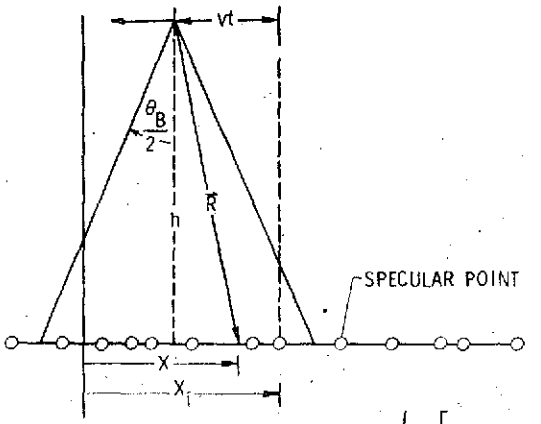

$$E_s^i(x,t) \sim \exp\left\{-j\left[2k_0\sqrt{(x-xi+vt)^2+h^2}\right]\right\} \sim \exp\left\{-j\left[\frac{2k_0(x-xi)vt}{h}+\frac{k_0V^2t^2}{h}\right]\right\}$$

Figure 1.

IMAGING RADAR SYSTEM

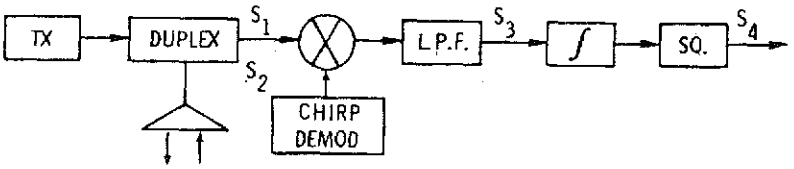

$$S_1 = \sum_i \exp\left\{-j\left[k_0(x-xi)\,vt/h + k_0v^2t^2/h - w_ct\right]\right\}$$

$$S_2 = \exp\left\{j\left[k_0v^2t^2/h - w_ct\right]\right\}$$

$$S_3 = \sum_i \exp\left\{-j\left[2k_0(x-xi)\,vt/h\right]\right\}$$

$$S_4 \sum P_i \left\{\frac{\sin\left[\frac{\pi(x-xi)}{x_0}\right]}{\left[\frac{\pi(x-xi)}{x_0}\right]}\right\}^2 \qquad x_0 = \frac{\lambda h}{2VT}$$

Figure 2.

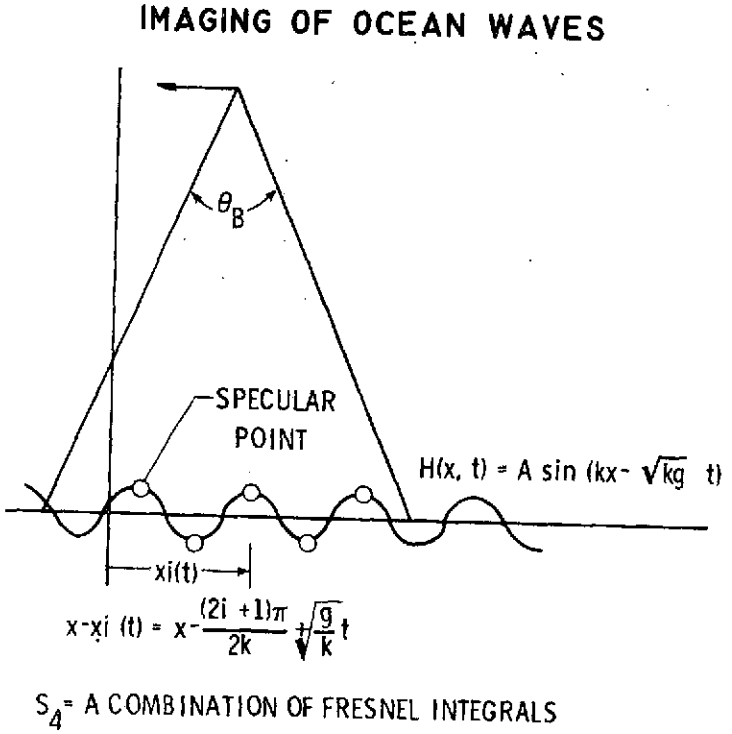

Figure 3.

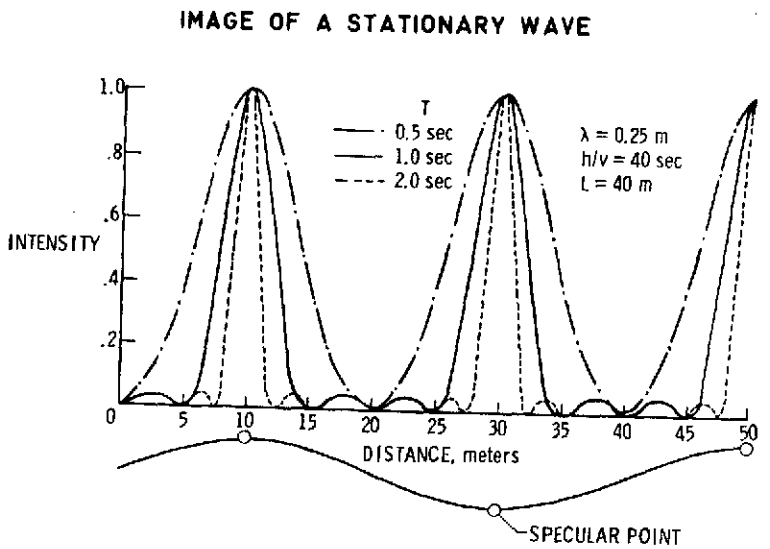

Figure 4.

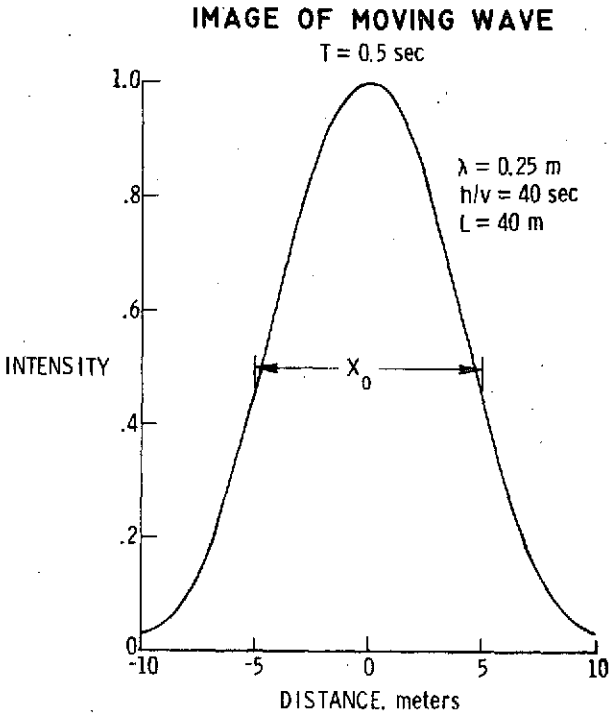

Figure 5.

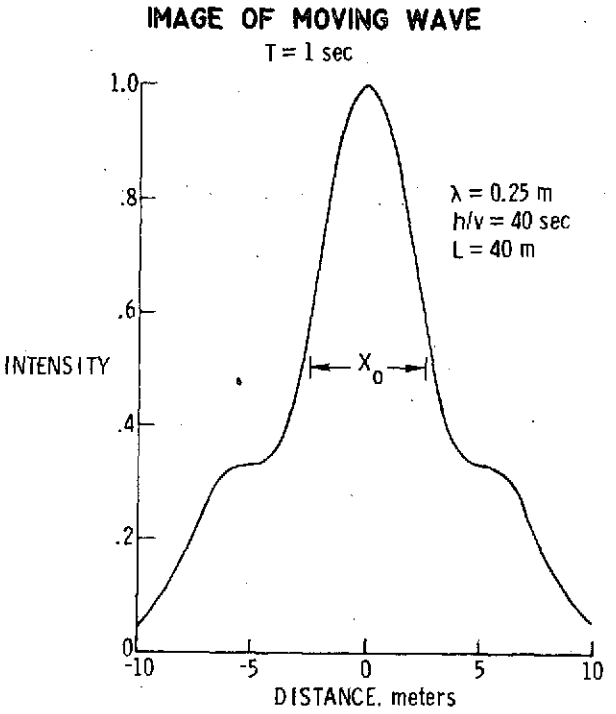

Figure 6.

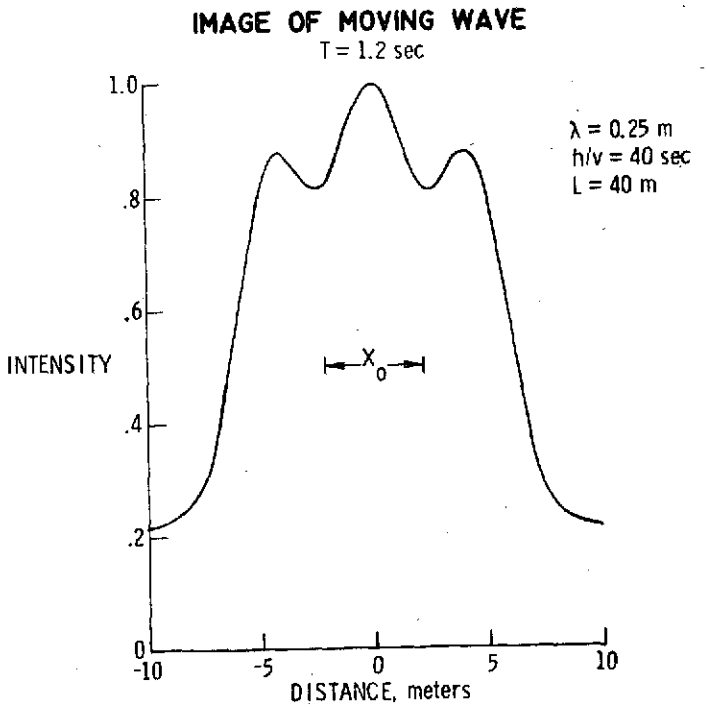

Figure 7.

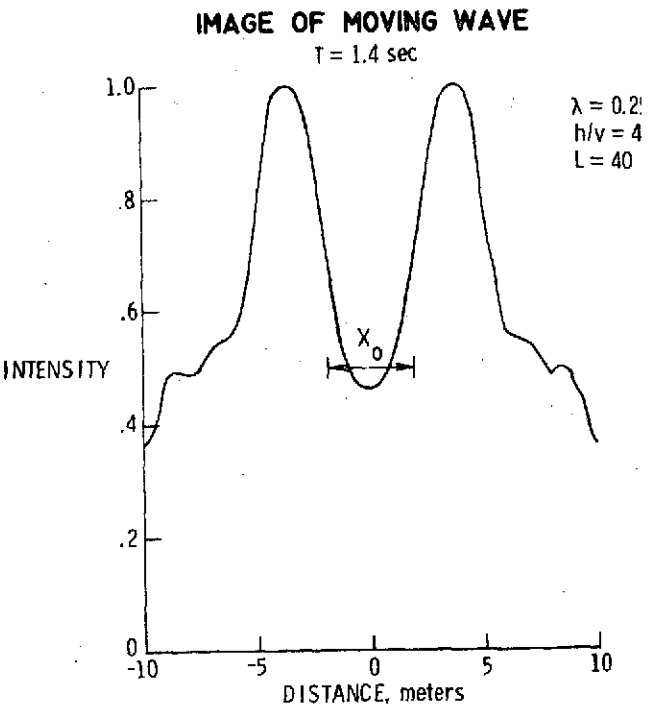

Figure 8.

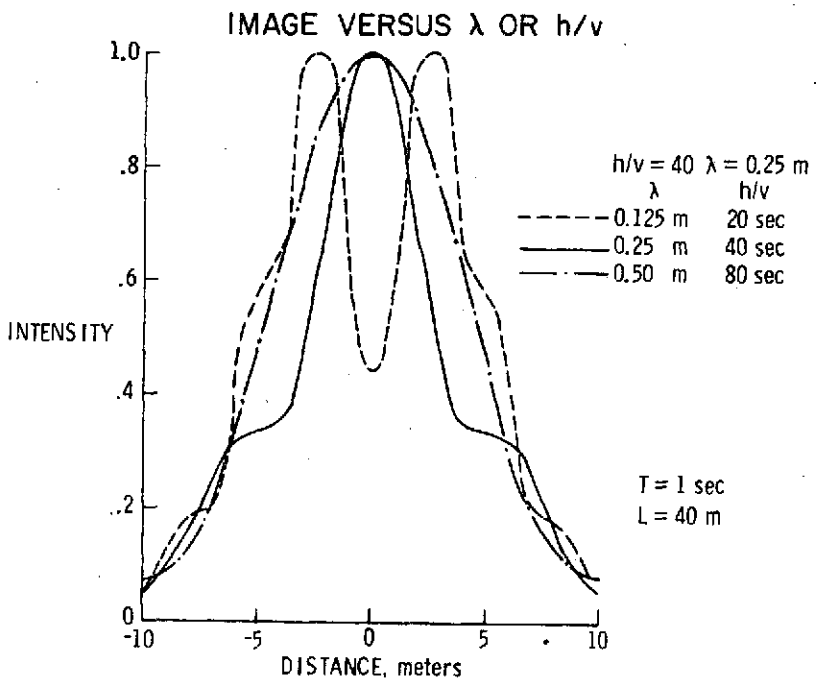

Figure 9.

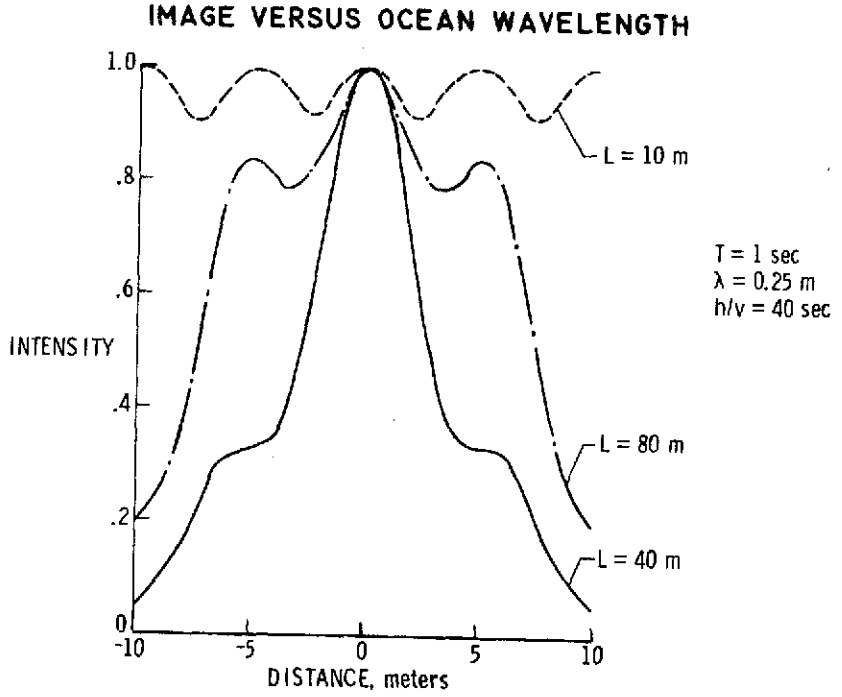

Figure 10.

SYSTEM OPTIMIZATION

A. HARDWARE IMPLEMENTATION

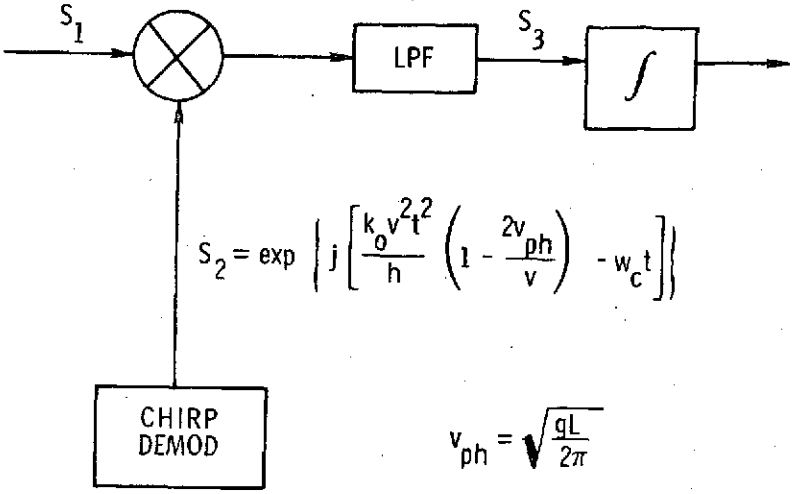

Figure 11.

SYSTEM OPTIMIZATION

B. SELECTION OF PARAMETERS

CRITERIA: $1.\ X_o \leq \frac{L_{min}}{4}$

$2.\ X_o \geq v_{ph_{max}} T$

WITH $X_o = \frac{\lambda h}{2vT}$ $\qquad v_{ph_{max}} = \sqrt{\frac{g L_{max}}{2\pi}}$

REPLACE $\geq$ BY $=$, ELEIMINATE T TO OBTAIN

$$\lambda\left(\frac{h}{v}\right) = \frac{1}{8}\sqrt{\frac{2\pi}{g}}\ \frac{L_{min}^2}{\sqrt{L_{max}}}$$

OR, $$\boxed{\lambda\left(\frac{h}{v}\right) = \frac{L_{min}^2}{10\sqrt{L_{max}}}}$$

Figure 12.